Resonant Transfer Excitation of Fluorine-Like Mo^{33+} Ion

Hassan Ramadan[a] and Sabbah Elkilany[b]

[a] Department of Basic Sciences, Faculty of Computer and Information Sciences, Ain Shams University, Cairo, Egypt
[b] Department of Mathematics, Faculty of Science, Kafr El-sheikh University, Kafr El-sheikh, Egypt

Reprint requests to H. R.; E-mail: hramadan@eun.eg

Z. Naturforsch. **65a,** 599 – 605 (2010); received January 7, 2009 / revised September 16, 2009

Dielectronic recombination (DR) cross sections ($\overline{\sigma}^{\mathrm{DR}}$) and rate coefficients (α^{DR}) for Mo^{33+} are calculated using the angular momentum average scheme (AMA). Moreover, the resonant transfer excitation followed by X-ray emission (RTEX) cross sections (σ^{RTEX}) for the collision of Mo^{33+} with H_2 and He targets are calculated and studied. The calculations of the cross sections are performed for both K- and L-shell excitations. A smooth change with the temperatures for α^{DR} is found for all kinds of excitations. The rates for K-shell excitation are very small in comparison with the rates for L-shell excitation. The RTEX cross sections for Mo^{33+} ions are obtained from their corresponding DR cross sections by the method of folding in the impulse approximation (IMA). σ^{RTEX} for the K-shell excitation shows two overlapped peaks which may be attributed to the two groups in this excitation process. The present calculations are considered as a database for future comparison with theoretical and experimental data using other coupling schemes. Multiple Auger channels are complicating the dependence of the cross sections on principal quantum numbers.

Key words: Atomic Data; Atomic Processes.

1. Introduction

Dielectronic recombination [1], is the dominant electron–ion recombination process in both photoionized and electron-collisional plasma. Extensive theoretical data are available for K-shell and L-shell excitations and have been presented in the recent years [2 – 4]. These data including radiative recombination (RR), have been used to provide new ionization balances for both electron-collisional [5] and photoionized plasmas [6]. In ion–atom (I/A) collisions, an electron may be captured from an atomic target by a positive projectile causing an excitation of the bound-state electrons of this projectile. This process is known as resonant transfer excitation (RTE). The resonant excited states of the projectile may be relaxed by emission of X-rays. This process is known as resonant transfer excitation followed by X-rays (RTEX). Brandt [7], showed that the RTEX in I/A collisions and dielectronic recombination (DR) in electron–ion (e/I) collisions are identical processes under the validity of conditions of impulse approximation (IMA). This means that RTEX and DR are two similar processes when the projectiles in I/A collisions are very fast. Moreover, Brandt proved that RTEX and DR cross sections are related and, successfully, he formalized such a mathematical relationship between RTEX and DR cross sections using the Compton profile of the momentum distribution of electrons in atomic He or molecular H_2 targets.

The present work deals with the calculations of the DR cross sections and rate coefficients for the collision of Mo^{33+} with a continuum electron. Then, by using these results, the RTEX cross sections σ^{RTEX} are calculated for the collision of Mo^{33+} ion (as a projectile) with H_2 and He as targets. The RTEX cross sections are studied for Mo^{33+} as a member of fluorine-like ions with K- and L-shell excitations. The DR cross sections are calculated using the adapted angular momentum average scheme (AMA) [8 – 11] in the isolated resonance approximation (IRA). The RTEX cross sections for Mo^{33+} ions are obtained from their corresponding DR cross sections by the method of folding in IMA. All bound state wave functions required in these calculations are generated by the single configuration Hartree-Fock (SCHF) program. σ^{RTEX}, for K-shell excitation, shows two peaks [12] in the fluorine-like isoelectronic sequence. However, these two peaks are not separated; it is easy to know the states responsible for each peak.

Moreover, $\sigma^{\rm RTEX}$ for L-shell excitation gives two separated peaks. The obtained results for $\sigma^{\rm RTEX}$ are consistent with the previous results in reference [11], for K-shell and L-shell excitations. In the recent years [13–17] many calculations have been done on many ions with other coupling schemes. These DR data are suitable for modelling of solar and cosmic plasma under conditions of collisional excitation.

2. Theory

The calculation of the energy dependent DR cross sections were carried out using the angular momentum average (AMA) scheme, which was used successfully in the recent study of DR [11] in the isolated resonance approximation (IRA). Then, in the impulse approximation (IMA), the DR cross sections are utilized to generate the RTEX cross sections for the collisions of Mo^{33+} with H_2 and with He atoms.

The DR process for Mo^{33+} ion can be represented schematically by three modes of excitations as follows:

Initial state	Intermediate doubly excited states		
	$1s2s^22p^6n\ell$	(a)	1s-Excitation
	$1s2s^22p^5n_1\ell_1\ n_2\ell_2$	(b)	1s-Excitation
$1s^22s^22p^5+e_c\ell_c$	$1s^22s2p^6n\ell$	(c)	2s-Excitation
	$1s^22s2p^5n_1\ell_1\ n_2\ell_2$	(d)	2s-Excitation
	$1s^22s^22p^4n_1\ell_1\ n_2\ell_2$	(e)	2p-Excitation

Many Auger channels are considered for the intermediate states (a), (b), and (d). Distorted wave calculations were performed to generate the approximate free electron, which is attached to each target state to yield the continuum state. In the calculations we consider $n \le 6$ and $0 \le \ell \le 4$, and the rest of states are derived by the method of extrapolation, see Hahn [12]. Moreover, for L-shell excitation, the $\Delta n = 0$ channel has not been considered, because of the difficulties in the calculation when there is a hole in the particular shell (case (c)).

In the DR process the electron–ion collision may be clarified schematically as follows:

$$e_{\rm c}+A^{q+} \underset{A_{\rm a}}{\overset{V_{\rm a}}{\longleftrightarrow}} \left(A^{(q-1)+}\right)^{**} \xrightarrow{A_{\rm r}} \left(A^{(q-1)+}\right)^{*}+\gamma, \quad (1)$$

where $e_{\rm c}$ is the continuum electron (projectile). The cross section is given by

$$\overline{\sigma}^{\rm DR} = \left[\frac{4\pi}{(p_{\rm e}a_0)^2}\right]\left(\frac{\rm Ry}{\Delta e_{\rm c}}\right)[\tau_0 V_{\rm a}(i\to d)]\,\omega(d)(\pi a_0^2), \quad (2)$$

where $p_{\rm e}$ is the momentum of the free electron. Moreover, $V_{\rm a}(i \to d)$ and $\omega(d)$ are the radiationless capture probability and fluorescence yield, respectively, given by

$$V_{\rm a}(i \to d) = \left(\frac{g_{\rm d}}{2g_{\rm i}}\right)\sum_{i_{\rm c}\ell_{\rm c}} A_{\rm a}(d \to i_{\rm c}\ell_{\rm c}) \quad (3)$$

and

$$\omega(d) = \frac{\sum_f A_{\rm r}(d \to f)}{\Gamma_{\rm a}(d)+\Gamma_{\rm r}(d)} \quad (4)$$

where $g_{\rm i}$ and $g_{\rm d}$ are the statistical weights of initial and intermediate states. $\Gamma_{\rm r}(d)$ and $\Gamma_{\rm a}(d)$ are the radiative and Auger decay widths of the d-state.

Equation (3) is related to the Auger emission probability while, (4) is related to both Auger ($A_{\rm a}$) and radiative ($A_{\rm r}$) probabilities. τ_0 is the atomic unit of time, and a_0 is the Bohr radius. $\Delta e_{\rm c}$ is chosen to be 10 Ry. The DR rate coefficients are given by

$$\overline{\alpha}^{\rm DR}(d) = \left[\frac{4\pi{\rm Ry}}{kT}\right]^{3/2}\left[a_0^3 V_{\rm a}(i \to d)\right]\omega(d)\exp\left[-\frac{e_{\rm c}}{kT}\right]. \quad (5)$$

The contribution to the high Rydberg states (HRS) is then estimated using the following formula [18]:

$$\sum_{m=n_{\rm c}}^{\infty}\bar{\alpha}^{\rm DR}(n) = \frac{1}{2}n_{\rm c}\left[1+\frac{1}{n_{\rm c}}+\frac{1}{2n_{\rm c}^2}\right] \cdot \left[\frac{n_{\rm c}-1}{n_{\rm c}}\right]^3 \overline{\alpha}^{\rm DR}(n_{\rm c}-1), \quad (6)$$

where $n_{\rm c}-1$ is the principal quantum number of the last detailed calculated level and corresponds here to $n = 6$.

The RTEX process can be represented schematically as

$$A^{q+}+B \xrightarrow{V_{\rm a}} (A^{(q-1)+})^{**}+B \xrightarrow{A_{\rm r}} (A^{(q-1)+})^{*}+B^{+}+\gamma. \quad (7)$$

The atom B in the ion–atom collision plays no role in the RTEX process.

The impulse approximation (IMA) is utilized to relate the RTEX cross section ($\overline{\sigma}^{\rm RTEX}$) to the DR cross section ($\overline{\sigma}^{\rm DR}$). The relationship between DR

Table 1. DR cross sections (in cm^2) for Mo^{33+} for 1s-, 2s-, and 2p-excitations.

1s-excitation			2s-excitation			2p-excitation		
$n\ell$	e_c(Ry)	$\overline{\sigma}^{DR} \times 10^{-23}$	$n_1\ell_1n_2\ell_2$	e_c(Ry)	$\overline{\sigma}^{DR} \times 10^{-22}$	$n_1\ell_1n_2\ell_2$	e_c(Ry)	$\overline{\sigma}^{DR} \times 10^{-22}$
3s	1131	1.736	$3s^2$	67	7.244	$3s^2$	53	3.256
3p	1136	9.983	3s4s	126	9.583	3s4s	113	1.047
3d	1143	2.164	3s5s	153	4.568	3s5s	140	0.381
4s	1190	0.611	3s6s	167	2.685	3s6s	154	0.188
4p	1192	3.645	3s3p	69	106.260	3s3p	56	49.364
4d	1195	1.056	3s4p	128	34.369	3s4p	115	9.848
5s	1216	0.284	3s5p	154	19.948	3s5p	141	3.540
5p	1217	1.742	3s6p	167	11.578	3s6p	154	1.727
5d	1219	0.568	3s3d	76	335.339	3s3d	63	17.212
6s	1230	0.157	3s4d	131	60.002	3s4d	118	1.832
6p	1231	0.974	3s5d	155	27.370	3s5d	142	0.644
6d	1232	0.335	3s6d	168	15.273	3s6d	155	0.318
$3s^2$	1316	0.826	$3p^2$	75	4.304	$3p^2$	62	0.124
3s3p	1319	2.270	3p4p	133	2.787	3p4p	119	20.289
$3p^2$	1324	5.410	3p5p	159	1.157	3p5p	145	11.845
3s3d	1326	0.251	3p6p	172	0.649	3p6p	159	7.587
3p3d	1331	1.912	3p3d	81	83.850	3p3d	67	560.595
$3d^2$	1338	0.127	3p4d	135	13.739	3p4d	122	112.453
3s4s	1376	0.661	3p5d	160	5.589	3p5d	146	45.309
3s4p	1379	0.883	3p6d	173	2.983	3p6d	159	32.735
3s4d	1381	0.125	3p4s	131	31.569	3p4s	118	11.582
3p4s	1381	0.820	3p5s	158	8.997	3p5s	144	5.080
3p4p	1383	3.676	3p6s	172	4.58	3p6s	158	2.733
3p4d	1386	0.952	$3d^2$	88	216.174	$3d^2$	74	830.664
3d4s	1387	0.087	3d4d	141	50.266	3d4d	127	249.581
3d4p	1389	0.655	3d5d	165	21.571	3d5d	151	112.317
3d4d	1392	0.102	3d6d	178	11.164	3d6d	165	61.199
3s5s	1403	0.335	3d4p	139	21.912	3d4p	125	95.525
3s5p	1404	0.436	3d5p	164	9.516	3d5p	151	36.040
3s5d	1406	0.066	3d6p	178	5.040	3d6p	164	18.018
3p5s	1408	0.378	3d4s	137	35.844	3d4s	123	2.882
3p5p	1409	1.887	3d5s	163	12.573	3d5s	150	1.104
3p5d	1410	0.504	3d6s	177	6.014	3d6s	164	0.556
3d5s	1414	0.041						
3d5p	1415	0.301						
3d5d	1416	0.055						
3s6s	1418	0.187						
3s6p	1418	0.247						
3s6d	1419	0.040						
3p6p	1422	1.066						
3p6s	1422	0.208						
3p6d	1423	0.296						
3d6p	1428	0.167						
3d6s	1428	0.022						
3d6d	1429	0.033						

and RTEX cross sections, following Brandt [7] and Hahn [12], is given by

$$\overline{\sigma}^{\mathrm{RTEX}} = \sqrt{\frac{M}{2E}} \Delta e_c J_B(p_z) \overline{\sigma}^{\mathrm{DR}}, \tag{8}$$

where M is the mass of the projectile ion of energy E, $J_B(p_z)$ is the Compton profile, and p_z is the z-component of the momentum.

3. Results and Discussion

3.1. DR Cross Sections

The dielectronic recombination cross sections for the collision of the projectile electron with the Mo^{33+} ion were calculated using the angular momentum average scheme (AMA).

(a) **K-shell excitation:** The DR cross sections are calculated for the collision of Mo^{33+} with a contin-

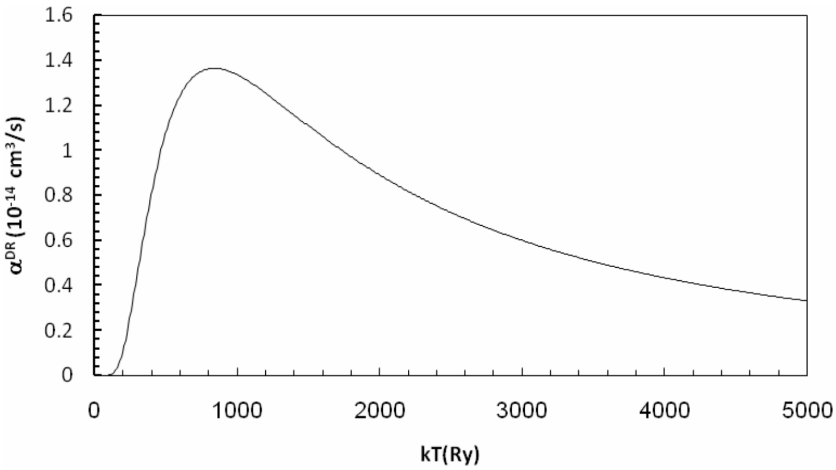

Fig. 1. DR rate coefficient for Mo^{33+} versus the temperature for K-shell excitation.

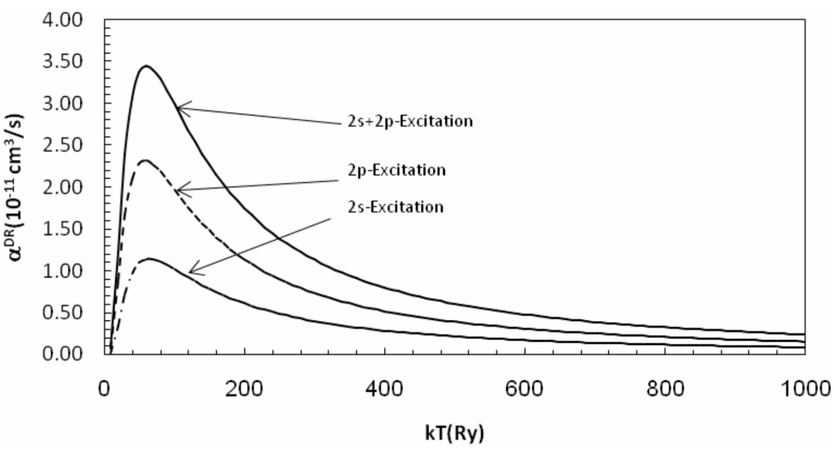

Fig. 2. Same as Figure 1 but for L-shell excitation.

uum electron, where the energy bin size is considered as $\Delta e_c = 10$ Ry. It is found that the dominant states in K-shell excitation are $1s2s^22p^6n\ell$ with $n = 3$ and 4, and $\ell = 0$, 1, and 2 and 3pnp states with $n = 3$ to 6, (Table 1).

(b) **L-shell excitation:** The DR cross sections for 2s- and 2p-excitation of $Mo^{33+} + e_c\ell_c$ are calculated. The energy bin size Δe_c is taken to be 10 Ry as in 1s-excitation. The DR cross sections for K- and L-shell excitation are presented in Table 1. It has to be noted that the DR cross sections for L-shell excitation are much larger (a factor of 10^3 for the dominant states) than that in the case of K-shell excitation. Whereas, as expected, the continuum energy e_c for K-shell excitation is much larger than that for L-shell excitation. Too many states are affected in the cross sections such as 3snp, 3snd, 3pnd, and 3dnd, but the most effective state in both excitations are $3d^2$ states.

3.2. DR Rates

The DR rate coefficients for Mo^{33+} are calculated in the isolated resonance approximation for the following two modes of excitations:

(a) **K-shell excitation:** The DR rates for Mo^{33+} when 1s-excitation is considered are given in Figure 1. α^{DR} for Mo^{33+} varies smoothly with kT. In addition, the DR rate coefficient has a peak at the energy $kT =$ 840 Ry.

(b) **L-shell-excitation:** The DR rates for Mo^{33+} with 2s-excitation are calculated in IRA approximation at different thermal energies of the continuum electrons. The contribution of high Rydberg states (HRS) are obtained at $n_c = 7$, i. e. the detailed calculations are stopped at $n = 6$, where A_a and A_r start to scale as $1/n^3$. Moreover, the DR rates are now calculated for the same ion, but with 2p-excitation using the same way as 2s-

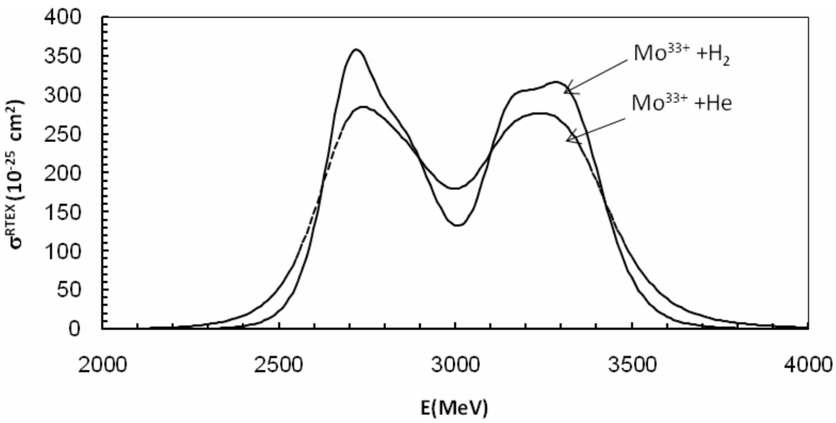

Fig. 3. Variation of RTEX cross section with the projectile energy E (MeV) in case of K-shell for the F-like Mo^{33+} ion in collision with both H_2 and He.

Table 2. DR rates α^{DR} values (in 10^{-12} cm^3/sec) from [13] and [17] in comparison with the present work for L-shell excitation for Mo^{33+} ion. (Total means $\Delta n = 0$ and $\Delta n \neq 0$ channels).

T (keV)	[13] Total	[18] $^2P_{3/2}$ $\Delta n \neq 0$	Present work AMA $\Delta n \neq 0$
0.10	25.0	0.167	1.00
0.30	24.4	12.5	12.20
0.50	34.1	24.4	30.70
0.80	38.2	31.4	35.00
1.00	37.4	32.1	34.00
1.50		29.2	28.00
2.00	26.4	24.9	23.00
3.00	18.5	17.9	16.00
5.00	10.6	10.5	9.00
7.00		7.03	6.00
9.00		5.10	4.00

excitation at different kT values of the projectile electrons. The variations of DR rates, α^{DR} (for both 2s- and 2p-excitation), with the thermal energies of the continuum electrons kT (Ry) are presented in Figure 2. From the figure it is clear that the L-shell excitation rate coefficients for Mo^{33+} are peaked around $kT = 60$ Ry. It has to be noted that the DR rate peak value for 2p-excitation is twice larger than the DR rate peak value for 2s-excitation. Moreover, the DR rates for L-shell excitation are much larger (a factor of 10^3) than the DR rates for K-shell excitation.

A good agreement is found between the present results for L-shell excitation with the results of Chen [17], which are shown in Table 2. The calculations of Chen were carried out in the isolated resonance approximation for temperatures in the range $0.001 \leq T \leq 9$ keV. The Auger and the radiative rates for each autoionizing state were computed explicitly using the multiconfiguration Dirac-Fock (MCDF) method in intermediate coupling and including configuration interaction. Moreover, the differences between the results of Fournier [13] and both, Chen [17] and the present work, may be attributed to the absence of the $\Delta n = 0$ channel.

3.3. RTEX Cross Sections

The RTEX cross sections are obtained from their corresponding DR cross sections for the following modes of excitations:

(a) **K-shell excitation:** Figure 3 shows the resonant transfer excitation cross sections for the collisions $Mo^{33+} + H_2$ and $Mo^{33+} + He$. The RTEX cross section shows two peaks corresponding to the two groups of excitation in case of K-shell excitations.

(b) **L-shell excitation:** The RTEX cross sections for the collision of $Mo^{33+} + H_2$ and $Mo^{33+} + He$ are presented in Figure 4.

It is clear that the collision with He gives a broader cross section than that with H_2. This reflects the nature of the Compton profile for the momentum distribution of the electrons in the He target, which is broader than that in the H_2 target. Two separate peaks are found in the case of L-shell excitation, which agree with the results obtained in [10], where the two-peak behaviour becomes more obvious for ions with $Z > 30$.

4. Conclusions

The present theoretical results for the DR cross sections, rate coefficients, and RTEX cross sections

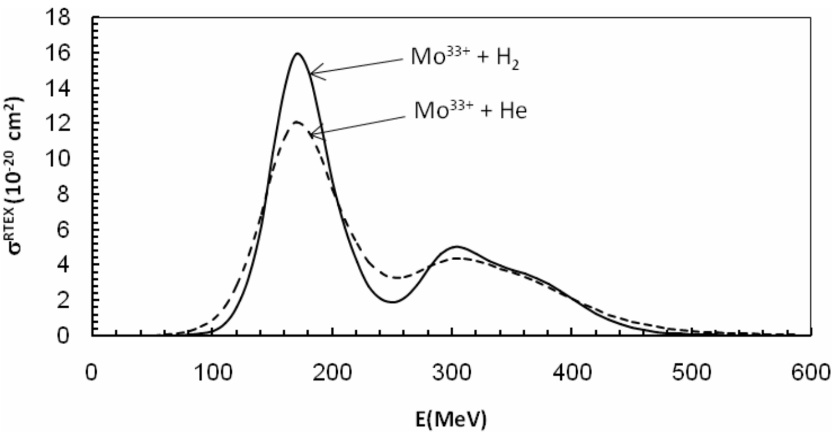

Fig. 4. Same as Figure 3 but for L-shell.

of fluorine-like Mo^{33+} ions forming neon-like Mo^{32+} ions are calculated using the angular momentum average scheme. The study is performed for both K-shell excitation and L-shell excitation. The results can be summarized as follows:

(a) **K-shell excitation**

- The dominant states in the DR cross sections are $1s2s^2 2p^6 n\ell$ with $n = 3$ and 4, and $\ell = 0$, 1, and 2 and $3pnp$ states with $n = 3$ to 6.
- The DR rates α^{DR} are varying smoothly with kT and peaked at the energy $kT = 840$ Ry.
- The RTEX cross sections for $Mo^{33+} + H_2$ and Mo^{33+} + He are found to have two peaks corresponding to the two groups of excitation.

(b) **L-shell excitation**

- The states 3s*n*p, 3s*n*d, 3p*n*d, and 3d*n*d, are the effective states in DR cross sections as well as the $3d^2$ states.
- The DR rates for 2p-excitation is twice as much as that for 2s-excitation. However, they both peaked around $kT = 60$ Ry.
- The DR rates for Mo^{33+} calculated in the present work and the calculation of Chen [17] (Table 2) are smaller than the same rates for Fournier [13], which is attributed to the neglecting of the $\Delta n = 0$ channel.
- The RTEX cross sections are showing two separate peaks and they are broader for the collision with He than the collision with H_2.
- The DR cross sections for K-shell excitation are much smaller than those for L-shell excitation by a factor of 10^3.
- The DR rate coefficients for L-shell excitation are larger than for K-shell excitation by a factor of 2×10^3.
- By the same way, the RTEX cross sections for L-shell excitation are larger than for K-shell excitation by a factor of about 10^4.
- This gives that the DR cross sections, rate coefficients, and RTEX cross sections are more efficient processes for outer shell excitations.

[1] A. Burgess, Astrophys. J. **139**, 776 (1964).
[2] O. Zatsarinny, T.W. Gorczyca, K.T. Korista, N.R. Badnell, and D.W. Savin, Astron. Astrophys. **426**, 699 (2004).
[3] O. Zatsarinny, T. W. Gorczyca, K. T. Korista, J. Fu, N.R. Badnell, W. Mitthumsiri, and D.W. Savin, Astron. Astrophys. **438**, 743 (2005); **440**, 1203 (2005).
[4] D.V. Lukić, M. Schnell, D.W. Savin, C. Brandau, E.W. Schmidt, S. Böhm, A. Müller, S. Schippers, M. Lestinsky, F. Sprenger, A. Wolf, Z. Altun, and N. R. Badnell, Astrophys. J. **664**, 1244 (2007).
[5] P. Bryans, N.R. Badnell, T.W. Gorczyca, J.M. Laming, W. Mitthumsiri, and D.W. Savin, Astrophys. J. Suppl. **167**, 343 (2006).
[6] T. Kalman and M. Bautista, Astrophys. J. Suppl. **133**, 221 (2001).
[7] D. Brandt, Phys. Rev. **A27**, 1314 (1983).
[8] H. Ramadan, A. Khazbak, and A. H. Moussa, Z. Naturforsch. **58a**, 346 (2003).
[9] H. Ramadan, Egypt J. Phys. **33**, 419 (2002).
[10] H. Ramadan and G. Omar, Sixth Radiation Physics Conference, Assiut, Egypt 2002, p. 27.
[11] G. Omar, H. Ramadan, and T. El-Kafrawy, Modern Trends in Physics Research, American Institute of Physics 2005, p. 79.

[12] Y. Hahn, Adv. Atom. Molec. Phys. **21**, 123 (1985).
[13] K. B. Fournier, M. Cohen, W. H. Goldstein, A. L. Osterheld, M. Finkenthal, M. J. May, J. L. Terry, M. A. Graf, and J. Rice, Phys. Rev. **A54**, 3870 (1996).
[14] E. W. Schmidt, S. Schippers, D. Bernhardt, A. Müller, J. Hoffmann, M. Lestinsky, D. A. Orlov, A. Wolf, D. V. Lukić, D. W. Savin, and N. R. Badnell, Astron. Astrophys. **492**, 265 (2008).
[15] D. Nikolić, T. W. Gorczyca, J. Fu, D. W. Savin, and N. R. Badnell, Nucl. Instr. Meth. **B261**, 145 (2007).
[16] Z. Altun, A. Yumak, I. Yavuz, N. R. Badnell, S. D. Loch, and M. S. Pindzola, Astron. Astrophys. **474** 1051 (2007).
[17] M. H. Chen, Phys. Rev. **A38**, 2332 (1988).
[18] H. H. Ramadan and Y. Hahn, Phys. Rev. **A39**, 3350 (1989).